

Striatum and pre-SMA facilitate decision-making under time pressure

Birte U. Forstmann^{a,1}, Gilles Dutilh^b, Scott Brown^c, Jane Neumann^d, D. Yves von Cramon^d, K. Richard Ridderinkhof^a, and Eric-Jan Wagenmakers^b

^aDepartment of Psychology, Amsterdam Center for the Study of Adaptive Control in Brain and Behavior, and ^bDepartment of Psychological Methodology, University of Amsterdam, 1018 WB, Amsterdam, The Netherlands; ^cSchool of Psychology, University of Newcastle, Newcastle 2308, Australia; and ^dDepartment of Cognitive Neurology, Max Planck Institute for Human Cognitive and Brain Sciences, 04103 Leipzig, Germany

Edited by Richard M. Shiffrin, Indiana University, Bloomington, IN, and approved September 25, 2008 (received for review June 18, 2008)

Human decision-making almost always takes place under time pressure. When people are engaged in activities such as shopping, driving, or playing chess, they have to continually balance the demands for fast decisions against the demands for accurate decisions. In the cognitive sciences, this balance is thought to be modulated by a response threshold, the neural substrate of which is currently subject to speculation. In a speed decision-making experiment, we presented participants with cues that indicated different requirements for response speed. Application of a mathematical model for the behavioral data confirmed that cueing for speed lowered the response threshold. Functional neuroimaging showed that cueing for speed activates the striatum and the pre-supplementary motor area (pre-SMA), brain structures that are part of a closed-loop motor circuit involved in the preparation of voluntary action plans. Moreover, activation in the striatum is known to release the motor system from global inhibition, thereby facilitating faster but possibly premature actions. Finally, the data show that individual variation in the activation of striatum and pre-SMA is selectively associated with individual variation in the amplitude of the adjustments in the response threshold estimated by the mathematical model. These results demonstrate that when people have to make decisions under time pressure their striatum and pre-SMA show increased levels of activation.

basal ganglia | fMRI | linear ballistic accumulator model | speed-accuracy tradeoff

Whether buying new shoes, participating in traffic, playing chess, or shooting basketball, one invariably faces the dilemma of when to stop deliberating and make a decision. In many situations, it is maladaptive to ponder over alternative courses of action for a very long time. In basketball, for instance, one has to shoot the ball before a defender can block the shot. However, decisions taken without sufficient thought may lead to poor results; a shot that is taken too hastily may not go in.

The foregoing example shows that decision-making involves a delicate balance between the competing demands of response speed and choice accuracy, a balance that is usually referred to as the speed-accuracy tradeoff (1). In the cognitive sciences, this tradeoff is thought to be modulated by a response threshold that determines the amount of diagnostic information that is required to make a decision and initiate an action (2, 3). Because the accumulation of diagnostic information takes time, high response thresholds lead to accurate, yet slow, decisions, and low response thresholds lead to fast yet error-prone decisions.

The behavioral consequences of the speed-accuracy tradeoff are both profound and predictable, and the tradeoff therefore constitutes one of the most important benchmark findings for formal models of decision-making (4, 5). In light of its ubiquity and impact, it is surprising that relatively little is known about the neural underpinnings of the speed-accuracy tradeoff (but see refs. 6 and 7). Despite a lack of empirical research, there is a lot of speculation that the basal ganglia may be critical to the speed-accuracy tradeoff (8–12). In their default state, the output

nuclei of the basal ganglia (i.e., the globus pallidus interna and the substantia nigra pars reticularis) send tonic inhibition to the thalamus, midbrain, and brainstem, preventing the premature execution of any action (13, 14). When cortical processes start to favor a certain course of action, it leads to activation of input nuclei of the basal ganglia (i.e., the striatum, consisting mainly of putamen and caudate), which, in turn, leads to selective suppression of the output nuclei, releasing the brain from inhibition and allowing the action to be executed (15).

Thus, the basal ganglia are thought to implement a generic action-selection mechanism that releases from inhibition those actions that are desirable and maintains inhibitory control over all others. The key hypothesis that is shared by recent neuro-computational models of decision-making (8–12) is that when people have to make decisions under time pressure the basal ganglia lessen their inhibitory control over the brain in a nonspecific fashion, thereby generally facilitating fast, but possibly premature, responses.

The goal of this article is to explore the neural correlates of decision-making under time pressure and test the widely held hypothesis that the basal ganglia modulate the speed-accuracy tradeoff. To this end, we experimentally manipulated the speed-accuracy balance in a speeded-up decision-making task and fitted a mathematical model to the behavioral data. Based on individual differences in the response threshold parameter of this model, functional neuroimaging data revealed that the striatum is involved in the process of setting the response threshold.

Results

In an experiment that consisted of a behavioral session and an fMRI session, 19 participants performed a standard “moving dots task” (16). This task requires a manual response to indicate whether a cloud of moving dots appears to move to the left or the right. Before each stimulus, a pseudorandomly presented cue indicated the level of speed stress: fast, accurate, or neutral (Fig. 1). After each response, participants received feedback consistent with the previously presented cue. In the speed and neutral conditions, participants saw the message “too slow” whenever they exceeded a response time criterion of 450 and 750 ms, respectively. In the neutral and accuracy conditions, participants saw the message “incorrect” whenever they made an incorrect response. This feedback procedure provided additional incentive

Author contributions: B.U.F., G.D., and E.-J.W. designed research; B.U.F., G.D., S.B., J.N., and E.-J.W. performed research; B.U.F., S.B., and E.-J.W. contributed new reagents/analytic tools; B.U.F., G.D., S.B., J.N., D.Y.v.C., and E.-J.W. analyzed data; and B.U.F., S.B., D.Y.v.C., K.R.R., and E.-J.W. wrote the paper.

The authors declare no conflict of interest.

This article is a PNAS Direct Submission.

¹To whom correspondence should be addressed. E-mail: b.u.forstmann@uva.nl.

This article contains supporting information online at www.pnas.org/cgi/content/full/0805903105/DCSupplemental.

© 2008 by The National Academy of Sciences of the USA

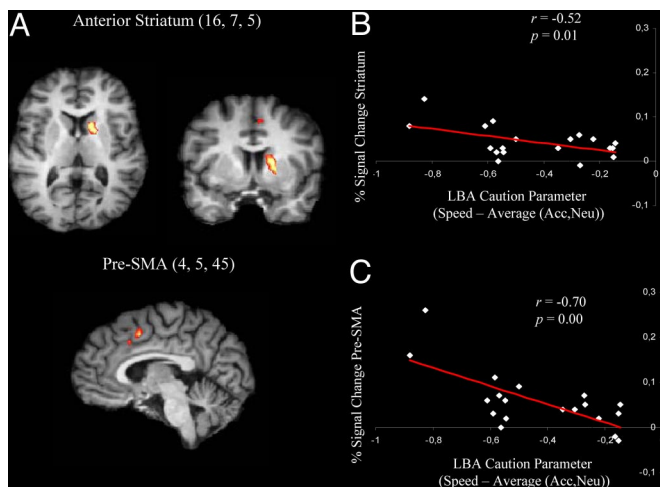


Fig. 3. Conjunction and correlation analyses. Activation maps averaged over 19 participants mapped onto an individual brain. Red labels indicate positive Z values. Coordinates are given in Talairach space. (A) Activation elicited in the conjunction analysis of both Speed vs. Accuracy and Speed vs. Neutral. (B) Association between the individual percent signal changes derived from the right anterior striatum and the individual changes in the LBA measure for response caution. (C) Association between the individual percent signal changes derived from the right pre-SMA and the individual changes in the LBA measure for response caution.

this choice as a race between 2 independent accumulators, illustrated in Fig. 2B. On each trial, the 2 accumulators begin with random activation values drawn from independent uniform distributions on $[0, A]$. After the stimulus is presented, activation increases in each accumulator at a rate that depends on the stimulus. For example, activation will generally increase quickly in the accumulator that corresponds to the correct response, but slowly in the accumulator that corresponds to the incorrect response. A response is triggered whenever the first accumulator reaches a fixed response threshold b . Thus, for any decision the observed response time is directly related to the time that the accumulators require to reach the threshold.

For parameter estimation, we used a constrained model in which response threshold b was the only parameter free to vary across cue conditions. We tried many other ways of constraining parameters, but settled on this simple scheme after considering the Bayesian Information Criterion for each design (see *SI Text* for details).

Fig. 2C shows that the model fits the data well, using a more complete way of illustrating the data than Fig. 2A. Instead of mean response times and error rates, this time we summarize the full response time distributions separately for correct and incorrect responses in each condition. Each distribution is summarized by using 5 quantile estimates that estimate the associated cumulative distribution functions. For each distribution, the slowest symbol (far right in Fig. 2C) represents the 90% quantile, the response time below which 90% of the data fall. In Fig. 2C, the next rightmost symbol represents the 70% quantile, the middle symbol represents the 50% quantile, which is just the median, and the leftmost symbols represent the 30% and 10% quantiles.

In Fig. 2C, the x axis shows the response time for the quantile estimates, and the y axis shows the associated proportion of data, which makes the graphs into defective cumulative distribution functions, which are commonly used in response time analysis (22). For example, in Fig. 2C *Left* (for data from the accuracy-emphasis condition) the 50% quantile (median) for correct responses was 493 ms. Overall accuracy in that condition was 87%. Half of the correct response times fall below the 50%

quantile, therefore 43.5% of all response times fall below this value, so the data point is plotted at $(x = 493, y = 0.435)$.

The quantile estimates support very detailed inspection of the data. For example, in the speed emphasis condition (Fig. 2C *Right*) the quantile estimates for the incorrect response times were all faster than the corresponding quantile estimates for correct response times, which replicates the usual finding that errors are fast, when speed is stressed (23). When accuracy was stressed, error response times tended to be about equal to correct response times, but also a little more variable (there was greater separation between the quantile estimates).

Comparison of the data (circles in Fig. 2C) with model predictions (lines and crosses in Fig. 2C) shows that the model fits the data very well. The predicted response probabilities are within 2.1% of the observed values for all conditions, and the predicted response quantiles for correct responses are always within 17 ms of the observed quantiles. Thus, application of the LBA model confirms that the behavioral effects of the experimental manipulation can be entirely accounted for by a change in the response threshold.

Individual Differences. Finally, and crucially, we combined the results from the mathematical modeling and the fMRI measurements (24) and correlated the LBA model parameters derived for each individual with the percentage signal change from both the anterior striatum and pre-SMA (see also *SI Text*). Specifically, for each participant and cue condition we calculated the ratio b/A as a measure of response caution. For consistency, we calculated contrasts between parameter estimates in the same way as for the fMRI data. Fig. 3B shows a significant negative correlation between the individual changes in the LBA measure for response caution and the individual percentage signal change derived from the right anterior striatum. Fig. 3C shows the same result for the right pre-SMA. In other words, when put under pressure to respond quickly, some participants adjust their response thresholds more than others. Those participants who have a relatively large decrease in response caution b/A also have a relatively large increase in activation for the right anterior striatum and right pre-SMA. The correlations between response caution b/A and anterior striatum and pre-SMA decrease somewhat when the datum with the highest percentage signal change is excluded (i.e., to $r = -0.48$ and -0.64 , respectively), but the results remain statistically significant (i.e., both $P < 0.05$).

We obtained almost identical results when we used a diffusion model (25) to account for the data; specifically, the correlation between EZ boundary separation variable and the hemodynamic response was $r = -0.41$ for the anterior striatum and -0.62 for the pre-SMA (both $P < 0.05$). This correspondence shows that our theoretical results generalize across different mathematical models.

The advantages of incorporating in the fMRI analysis the parameters of a mathematical model (instead of more direct summaries of the observed data) are further underscored when one considers the selective nature of the association between individual differences in the hemodynamic response and those in the response caution measure derived from the LBA model. For instance, the association between the hemodynamic response and LBA response caution is much more consistent than the association between the hemodynamic response and mean response time or proportion correct; in fact, for the latter 2 measures the only significant relation was between proportion correct and activation in the pre-SMA ($r = -0.59, P = 0.007$). Also, individual differences in parameters of the LBA model other than response caution (e.g., drift rate) did not correlate with individual differences in the hemodynamic response, further attesting to the selectivity of the association reported in Fig. 3B and C.

Discussion

Our fMRI analysis showed that when people make decisions under time pressure, it is accompanied by a focused activation in anterior striatum and pre-SMA. The cognitive interpretation of this result was corroborated by fitting the LBA model to the data and demonstrating an association between the LBA model parameters and individuals' hemodynamic responses. These findings confirm that the striatum is instrumental in adjusting response caution, an assumption from several neuro-computational models of decision-making that has so far evaded experimental scrutiny. Our results are particularly consistent with the model of Lo and Wang (12), who have argued that, in an oculomotor task, time pressure causes an increase in activation in the striatum, which then acts to disinhibit the oculomotor action execution system.

Our results are also partly consistent with recent work by Ivanoff *et al.* (6) and van Veen *et al.* (7). Ivanoff *et al.* reported that speed emphasis leads to activation in striatum and pre-SMA and in more frontal areas. Van Veen *et al.* also reported activation of many brain areas, including the striatum, premotor areas of the frontal lobe, and the dorsolateral prefrontal and left parietal cortices. The differences between these results and ours may be caused by differences in task, design, computational modeling, and research focus. We tentatively suggest that the relatively broad activation patterns in prefrontal cortex could come about through the use of a suboptimal procedure in which cues precede not just single trials, but entire blocks of trials.

The basal ganglia is a complicated brain structure that is important for reinforcement learning (26), voluntary motor behavior (27), and motor dysfunctions associated with Parkinson's and Huntington's disease (28). The connections between the pre-SMA and the basal ganglia, more specifically the anterior striatum, render this circuit optimally suitable for modulating action readiness. Accordingly, our work suggests that the striatum, in interaction with the pre-SMA, may also be important in the crucial everyday task of maintaining a balance between fast decisions and accurate decisions.

Materials and Methods

Participants. Twenty healthy volunteers participated for a small monetary reward of 8 euros. All participants signed a consent form before the scanning session. All participants had normal or corrected-to-normal vision, and none of them had a history of neurological, major medical, or psychiatric disorders. The data of 1 participant were excluded from the analysis because of movement. The remaining 19 participants (10 women, median age = 25.5, SD age = 3.08) were all right-handed, as confirmed by the Edinburgh Inventory (29).

Behavioral Task. In the present study we used the moving-dots task, popular in neuroscience and research with primates (16); for an overview see ref. 30. Participants were required to decide whether a cloud of dots appeared to move to the left or to the right (Fig. 1). Of 120 dots, 60% moved coherently, and 40% moved randomly. Participants indicated their response by pressing 1 of 2 spatially compatible buttons with their left or right index finger. A cue (SN for schnell, i.e., fast; NE for neutral; and AK for accurate) instructed participants to adopt different levels of cautiousness on a trial-by-trial basis. The cues were pseudorandomly intermixed. At the end of each trial, participants received feedback that depended on the previously presented cue. In the speed and neutral conditions, participants saw the message "zu langsam" (too slow) whenever they exceeded a response time criterion of 450 and 750 ms, respectively. In the neutral and accuracy conditions, participants saw the message "falsch" (incorrect) whenever they made an incorrect response. This feedback procedure provided an additional incentive for participants to adopt different levels of response caution in response to the different cues.

Timing of fMRI Experiment. The timing of the sequence of trials was triggered from the MRI control every 10 s. The trials started with a variable oversampling interval of 0, 500, 1,000, or 1,500 ms to obtain an interpolated temporal resolution of 500 ms. During the variable oversampling interval a fixation cross was presented. Participants were asked to maintain fixation. Then 1 of the 3 cues was presented in the middle of the screen for 4,800 ms (Fig. 1). Cue

presentation was followed by a jittered interval between 0 and 1,500 ms in steps of 500 ms. The imperative stimulus (i.e., the moving dot pattern) was presented for 1,500 ms and followed by 350 ms of feedback.

The experiment consisted of 240 trials including 24 null events that were pseudorandomly interspersed. The null events were included to compensate for the overlap of the bloodoxygenation level-dependent response between adjacent trials. The experiment lasted ≈ 40 min. Every block started out with 2 dummy trials that were excluded from further analysis.

Details of the fMRI procedure and analyses can be found in *SI Text*.

Behavioral Session for the Estimation of Response Threshold. Two days before the scanning session, each participant performed the task outside the MRI scanner for ≈ 40 min. This process yielded sufficient data for the reliable estimation of the response boundary thresholds by using the LBA model as described. The trial timing of the task for this behavioral session was modified to maximize the number of observations, i.e., the cue-stimulus interval was set to 500 ms and there was no variable jitter at the beginning of the trial. Moreover, cue and stimulus were each presented for 1,000 ms, and there were no null events interspersed. The behavioral session features a total of 840 trials, equally distributed over the 3 conditions.

Analysis Using a Mathematical Model for Response Speed and Accuracy. We analyzed the data by using the LBA model (21). The data were also analyzed with the EZ-diffusion model (25), yielding qualitatively identical results. Each time participants were presented with a stimulus, they were required to choose 1 of 2 response options, either left or right. The LBA model represents this choice as a race between 2 independent accumulators, illustrated in Fig. 2B. On each trial, the 2 accumulators begin with random activation values drawn from independent uniform distributions on $[0, A]$. After the stimulus is presented, activation increases in each accumulator at a rate of d units per millisecond, where we call d the drift rate. The drift rate is a random sample from a normal distribution, with variance s^2 and a mean value that depends on the stimulus (for example, the drift rate for the accumulator that responds left will be large when the stimulus strongly suggests that response, and small when the stimulus suggests the other response). A response is triggered whenever the first accumulator reaches a fixed response threshold, b , and the time taken for that response is the time taken to reach the threshold plus a constant offset time t_0 .

The predicted response time distributions and associated response probabilities for the LBA can be specified in closed forms (21) and used to calculate likelihood functions when fitting the model to data from the behavioral phase of the experiment. We performed similar analyses on the entire dataset, including data collected in the magnet. The results were similar, but noisier because of increased response variability in the scanner; in particular, there were many anticipatory responses. To fit the data, we first removed observations with response times < 250 ms on the grounds that these observations were unlikely to have arisen from the decision process of interest. This trimming resulted in the removal of 105 observations, or only 0.3% of the data. We then estimated response time quantiles corresponding to 0.1, 0.3, 0.5, 0.7, and 0.9 cumulative probabilities. The response time quantile corresponding to, say, probability 0.7 is just that response time below which 70% of the data fall, and these quantiles can be used to succinctly describe response time distributions. We calculated the 5 quantile estimates separately for each participant in 12 experimental conditions (3 response caution conditions crossed with 2 responses and 2 stimuli). For fixed model parameters, the probability mass predicted by the LBA model for each interquantile bin was computed, and they were combined by using the quantile maximum product method (31, 32). The parameters were then adjusted to maximize the probability product, independently for each participant, using the simplex algorithm (33).

For a decision between 2 responses, the LBA model appears to have 7 parameters: t_0 , A , b , and means and standard deviations for the drift rate distributions for both left (d_L and s_L) and right (d_R and s_R) responses. For reasons of plausibility and parsimony, we limited these parameters considerably. We constrained the offset time (t_0) and the range of the start point distribution (A) to be fixed across all conditions, and we allowed the response threshold (b) to vary only with response caution. For a given stimulus class (left or right) we used an identical standard deviation for the drift rate distributions for both responses (left and right) and constrained the means of the drift rate distributions to add to one.

The value of 1 was chosen arbitrarily, to enforce a scaling property of the LBA model. This process resulted in 2 free parameters for drift rates, d and s , which we estimated separately for left-moving and right-moving stimuli. These constraints allowed the model to predict the 12 separate distributions of response times by using just 9 free parameters: t_0 , A , b_S , b_A , b_N (for speed, accuracy, and neutral conditions), and d_L , s_L , d_R , s_R (for left and right stimuli).

We tried many other designs for constraining parameters, such as allowing t_0 to vary with response caution or fixing the drift rate parameters across stimulus classes. All reasonable designs resulted in similar goodness-of-fit for the model and in qualitatively consistent results for parameter analyses.

Fig. 2C shows that the model fits the data very well. The predicted response probabilities are within 2.1% of the observed values for all conditions. The response quantiles predicted by the model are within 17 ms of the observed quantiles for all distributions associated with correct responses (see *Results*). The misses are larger for distributions associated with incorrect responses, up to 106 ms, primarily because the data for incorrect responses were fewer and more variable than for correct responses. The model also captures all of the important qualitative trends in the data. For example, both correct and incorrect response time distributions are faster (closer to the left) in the speed condition than in the other 2 response caution conditions. Also, the response accuracy is lower in the speed condition than in the other 2 conditions (in Fig. 2C the y-axis probabilities for the 2 distributions in the speed condition are closer together than in the other conditions).

The LBA model captures response caution through the relative sizes of the response threshold (b) and the upper end of the distribution of starting points (A). When the response threshold is set close to start point distribution (i.e., when $b \approx A$) responses are very fast, but are often incorrect. However, when

$b \gg A$, the model predicts longer accumulation times and so there is a reduced effect of different starting points for the accumulators, which leads to greater accuracy at the expense of slower responses. As a measure of response caution, we calculated the ratio b/A separately for each participant and separately for the 3 response caution conditions. The means (and standard errors) for these were 1.66 (0.072), 1.54 (0.069), and 1.17 (0.057) in the accuracy, neutral, and speed conditions, respectively. The increase in response caution when moving from speed emphasis to neutral and accuracy emphasis conditions confirms that the experimental condition had the desired effect. The relative similarity of the response caution measures in the neutral and accuracy conditions confirms the conclusion we drew from the descriptive analyses; that participants treated these 2 conditions similarly. Therefore, and for consistency, when comparing our model analyses with fMRI data, we averaged the estimates from the accuracy and neutral conditions and made a single contrast, subtracting the response caution measure in the combined conditions from the response caution measure in the speed condition.

ACKNOWLEDGMENTS. We thank Ruud Wetzels for help in programming the moving dots task and Mandy Naumann for assistance with the fMRI measurements. This work was supported by National Institutes of Health Grant R01 MH74457 and Cognition Pilot, Vidi, and Vici grants from the Netherlands Organization for Scientific Research.

1. Wickelgren WA (1977) Speed-accuracy tradeoff and information processing dynamics. *Acta Psychol* 41:67–85.
2. Bogacz R, Brown E, Moehlis J, Holmes P, Cohen JD (2006) The physics of optimal decision making: A formal analysis of models of performance in two-alternative forced choice tasks. *Psychol Rev* 113:700–765.
3. Ratcliff R (1978) A theory of memory retrieval. *Psychol Rev* 85:59–108.
4. Ratcliff R, Smith PL (2004) A comparison of sequential sampling models for two-choice reaction time. *Psychol Rev* 111:333–367.
5. Wagenmakers EJ, Ratcliff R, Gomez P, McKoon G (2008) A diffusion model account of criterion shifts in the lexical decision task. *J Memory Language* 58:140–159.
6. Ivanoff J, Branning P, Marois R (2008) fMRI evidence for a dual process account of the speed-accuracy tradeoff in decision-making. *PLoS One* 3:e2635.
7. van Veen V, Krug MK, Carter CS (2008) The neural and computational basis of controlled speed-accuracy tradeoff during task performance. *J Cognit Neurosci*, in press.
8. Bogacz R, Gurney K (2007) The basal ganglia and cortex implement optimal decision making between alternative actions. *Neural Comput* 19:442–477.
9. Brown JW, Bullock D, Grossberg S (2004) How laminar frontal cortex and basal ganglia circuits interact to control planned and reactive saccades. *Neural Networks* 17:471–510.
10. Frank MJ (2006) Hold your horses: A dynamic computational role for the subthalamic nucleus in decision making. *Neural Networks* 19:1120–1136.
11. Gurney K, Prescott TJ, Wickens JR, Redgrave P (2004) Computational models of the basal ganglia: From robots to membranes. *Trends Neurosci* 27:453–459.
12. Lo CC, Wang XJ (2006) Cortico-basal ganglia circuit mechanism for a decision threshold in reaction time tasks. *Nat Neurosci* 9:956–963.
13. Chevalier G, Vacher S, Deniau JM, Desban M (1985) Disinhibition as a basic process in the expression of striatal functions. I. The striato-nigral influence on tecto-spinal/tecto-diencephalic neurons. *Brain Res* 334:215–226.
14. Deniau J, Chevalier G (1985) Disinhibition as a basic process in the expression of striatal functions. II. The striato-nigral influence on thalamocortical cells of the ventromedial thalamic nucleus. *Brain Res* 334:227–233.
15. Mink JW (1996) The basal ganglia: Focused selection and inhibition of competing motor programs. *Progr Neurobiol* 50:381–425.
16. Britten KH, Shadlen MN, Newsome WT, Movshon JA (1992) The analysis of visual motion: A comparison of neuronal and psychophysical performance. *J Neurosci* 12:4745–4765.
17. Nichols T, Brett M, Andersson J, Wager T, Poline J-B (2005) Valid conjunction inference with the minimum statistic. *NeuroImage* 25:653–660.
18. Alexander GE, Crutcher MD (1990) Functional architecture of basal ganglia circuits: Neural substrates of parallel processing. *Trends Neurosci* 13:266–271.
19. Inase M, Tokuno H, Nambu A, Akazawa T, Takada M (1999) Corticostriatal and corticosubthalamic input zones from the presupplementary motor area in the macaque monkey: Comparison with the input zones from the supplementary motor area. *Brain Res* 833:191–201.
20. Shima K, Tanji J (1998) Both supplementary and presupplementary motor areas are crucial for the temporal organization of multiple movements. *J Neurophysiol* 80:3247–3260.
21. Brown SD, Heathcote AJ (2008) The simplest complete model of choice reaction time: Linear ballistic accumulation. *Cognit Psychol*, in press.
22. Ratcliff R, Tuerlinckx F (2002) Estimating parameters of the diffusion model: Approaches to dealing with contaminant reaction times and parameter variability. *Psychonomic Bulletin Rev* 9:438–481.
23. Ratcliff R, Rouder JN (1998) Modeling response times for two-choice decisions. *Psychol Sci* 9:347–356.
24. Forstmann BU, van den Wildenberg WPM, Ridderinkhof KR (2008) Neural mechanisms, temporal dynamics, and individual differences in interference control. *J Cognit Neurosci* 20:1854–1865.
25. Wagenmakers EJ, van der Maas HJL, Grasman RPPP (2007) An EZ-diffusion model for response time and accuracy. *Psychonomic Bulletin Rev* 14:3–22.
26. Graybiel AM (2005) The basal ganglia: Learning new tricks and loving it. *Curr Opin Neurobiol* 15:638–644.
27. Houk JC, Davis JL, Beiser DG, eds (1998) *Model of Information Processing in the Basal Ganglia* (MIT Press, Cambridge, MA), 2nd ed.
28. Wichmann T, DeLong MR (1996) Functional and pathophysiological models of the basal ganglia. *Curr Opin Neurobiol* 6:751–758.
29. Oldfield RC (1971) The assessment and analysis of handedness: The Edinburgh Inventory. *Neuropsychologia* 9:97–113.
30. Gold JI, Shadlen MN (2007) The neural basis of decision making. *Annu Rev Neurosci* 30:535–574.
31. Heathcote A, Brown SD (2004) Reply to Speckman and Rouder: A theoretical basis for QML. *Psychonomic Bull Rev* 11:577–578.
32. Heathcote A, Brown SD, Mewhort DJK (2002) Quantile maximum-likelihood estimation of response time distributions. *Psychonomic Bull Rev* 9:394–401.
33. Nelder JA, Mead R (1965) A simplex algorithm for function minimization. *Comput J* 7:308–313.